

# Analysis of Airfoils Modifications on Horizontal Axis Wind Turbine Blades

Carlos M. Guzmán Claudio  
Master of Engineering in Mechanical Engineering  
Dr. Moisés Angeles  
Department of Mechanical Engineering  
Polytechnic University of Puerto Rico

**Abstract** — This project investigates the combination of upper surface dimples and trailing edge serrations of a 3D thin airfoil and their effect on aerodynamic performance. Dimples are known to reduce a golf ball's drag while a serrated trailing edge is known to reduce noise. A flatback design is also studied to see if its properties apply to a thin airfoil. The airfoil in the present study is NREL S825, to be 3D-printed with six combinations of the proposed modifications and tested in a wind tunnel. This study has found that the combination of dimples, flatback, and serrations has increased the maximum lift coefficient by 9.85%; however the maximum lift-to-drag ratio has been reduced by 14.4%.

**Key Terms** — Dimples, Flatback, NREL S825, Serrated Trailing Edge.

## INTRODUCTION

The objective of this work is to study the behavior of a wind turbine blade when it is modified with upper surface dimples, flatback trailing edge, and trailing edge serrations. These modifications should help improve the performance of a blade by reducing the drag wake. The dimples should act as vortex generators, delaying boundary layer separation; the flatback shape may reduce the pressure gradient along the surface of the blade; and the serrations could break up vortices behind the blade by forcing the wake to dissipate energy.

The combination of these modifications would give a better understanding of how to approach designing future wind turbine blades for higher efficiency.

One modification consists in to use dimples on the airfoil surface. In a golf ball, dimples act as vortex generators. These vortices force the air around the ball to transition from laminar to turbulent at an earlier phase relative to a smooth ball. The turbulence mixes higher velocity air into the surface of the ball, delaying the boundary layer separation, as visualized in Figure 1. This delay then reduces the wake drag of the ball, thus allowing the ball to go farther and higher than a smooth counterpart [1].

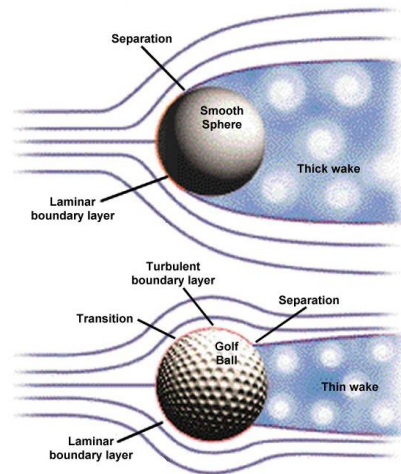


Figure 1

### Flow Separation on A Sphere and a Golf Ball

There is an effect on airfoil performance when introducing a variety of dimples to the upper surface of the wing, such as circular and squared shaped dimples [2]. Notably, having either inwards or outwards dimple on the upper surface delays flow separation from the aircraft wing, resulting in increased coefficient of lift and decreased coefficient of drag [3]. Reference [4] observed that a more continuous drop in pressure is produced by the dimpled surface, allowing the airfoil to stall at higher angles than the smooth counterpart. A symmetrical

airfoil at an angle of attack of  $20^\circ$  with its upper surface mostly covered in dimples decreased the drag coefficient by 20.5% (Figure 2) and increased its lift coefficient by 34.19% (

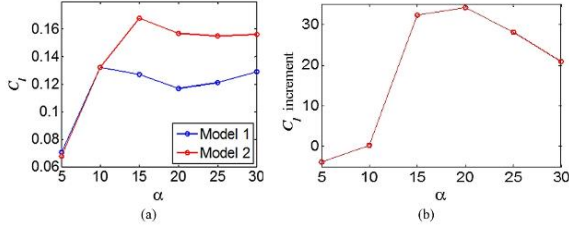


Figure 3) [5].

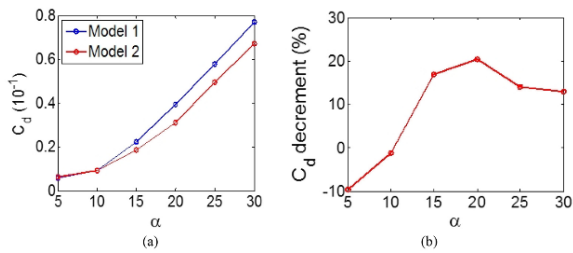


Figure 2

(a) Drag Coefficient versus Angle of Attack and (b) Drag Coefficient Decrement of Model 2 with Respect to Model 1 versus Angle of Attack [5]

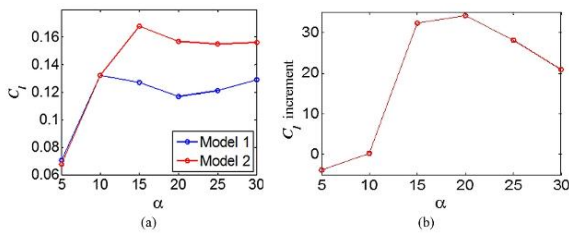


Figure 3

(a) Lift Coefficient versus Angle of Attack and (b) Lift Coefficient Increment of Model 2 with Respect to Model 1 versus Angle of Attack [5]

The next modification involves a flatback trailing edge. The idea behind blunting the trailing edge is to improve structural integrity of the root region of the blade by increasing the cross-sectional area, resulting in greater buckling resistance. Blunting the trailing introduces an increased base drag at higher Reynolds Number, so it is best used for the root region of the blade. It also comes with the benefit of increased lift performance and greater resistance to leading edge soiling [6].

One way to generate a flatback airfoil is to cut off, truncating, a segment of the trailing edge of the airfoil. Another way to create a flatback airfoil is to increase the thickness of the trailing edge while maintaining the mean camber line of the airfoil (Figure 6). Thickness must be added along the camber line to prevent adverse boundary layer effects. In reference [6], the author studied the effects of modifying a 35% thickness-to-chord ( $t/c$ ) airfoil in the various forms. A comparison of these airfoils can be seen in Figure 4:

- The base TR-35 sharp-trailing edge airfoil
- TR-35.80 truncated at  $x/c = 80\%$ , resulting  $t/c = 44\%$  and  $t_{TE}/c = 10\%$
- TR-44 a sharp-trailing edge TR-35 airfoil thickened to  $t/c = 44\%$
- TR-35-10 is a blunt trailing edge airfoil with a  $t/c = 35\%$  and  $t_{TE}/c = 10\%$

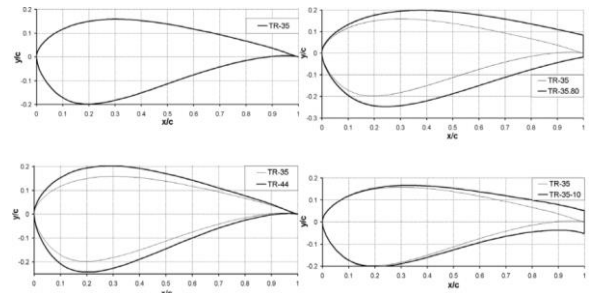


Figure 4

TR Series Airfoils [6]

This truncation method proved to hinder the performance of the airfoil due to the loss of maximum camber, as seen in Figure 5. The TR-44 airfoil is too thick for practical use. The truncated TR-35.80 resulted with a higher maximum lift, but with a significantly reduced lift slope. The TR-35-10 possesses superior lift performance along the entire angle-of-attack range.

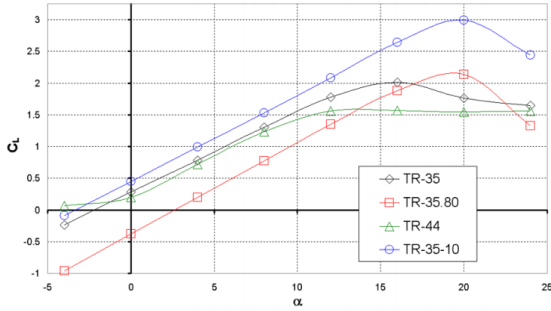


Figure 5

Effect of Trailing Edge Modification on Lift,  $Re = 4.5e6$  [6]

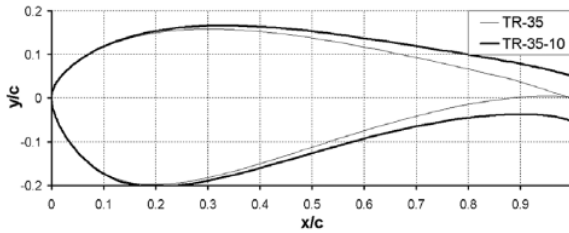


Figure 6

Blunt Trailing-edge Airfoil with  $T/c=35\%$ ,  $T_w/c=10\%$  [6]

The subsequent modification proposed is the serrating the trailing edge which comes from a need to reduce the aerodynamic noise profile of the blade, mainly from the tip, as its periodic nature can become an annoyance to nearby residences [7]. A variety of serrations can be generated, such as rectangular, sawtooth, and M-shaped. The most common of these is the sawtooth shape. They serve to induce a span-wise pressure gradient, forcing vortices to collide and breakup. Figure 7 and Figure 8 show a few example comparisons of different kinds of possible serrations and their effects on base drag reduction. Figure 7 shows how an M-Shaped serration has lower base pressure losses over a rectangular serration. Figure 8 shows how the differences in angle on a sawtooth serration impact the overall base drag on a flatback blade.

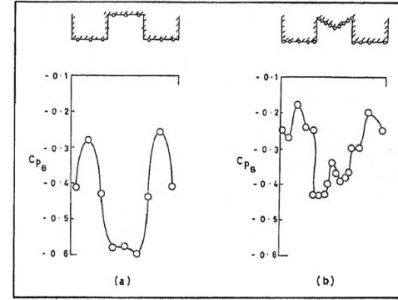


Figure 7

Base Pressure of a Slotted and an M-shaped Serrated Trailing Edge [9]

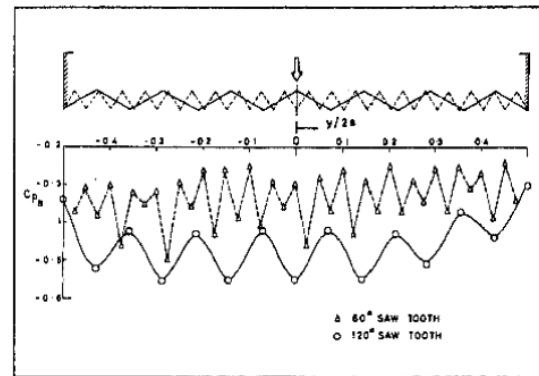


Figure 8

Base Pressure of A 60° and 120° Sawtooth Serrated Trailing Edge [9]

In reference [8] two airfoils, namely a NACA 0012 and a NACA 65(12)-10, were studied in a wind tunnel with a variety of trailing edge forms. These forms include a sawtooth, sinusoidal, and slotted sawtooth serrations of various frequencies. The study shows that, for the NACA 65(12)-10, serrations don't significantly change the drag coefficient and the lift coefficient reduces up to 15% between angles of  $-5^\circ$  to  $10^\circ$ , however at higher angles the drag increases with larger wavelength serrations. Figure 9 shows these results for various sawtooth serrations. The sinusoidal serration has similar performance to the sawtooth serration. The slotted-sawtooth resulted in up to 30% reduction in lift coefficient over the entire range on angles studied.

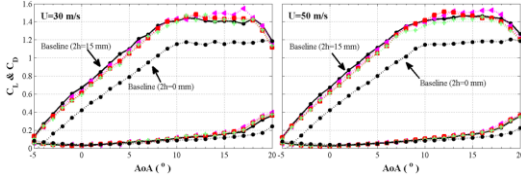


Figure 9

**Lift and Drag Coefficients for A NACA 65(12)-10 Airfoil Fitted with Different Sawtooth Serrations [8]**

A follow up study [9] investigated the wake development of the previously mentioned airfoil serrations. It found that for the NACA 65(12)-10, the overall wake development for both the sawtooth and slotted sawtooth serrations is less turbulent due to the interactions of the tip-flow and the root-flow.

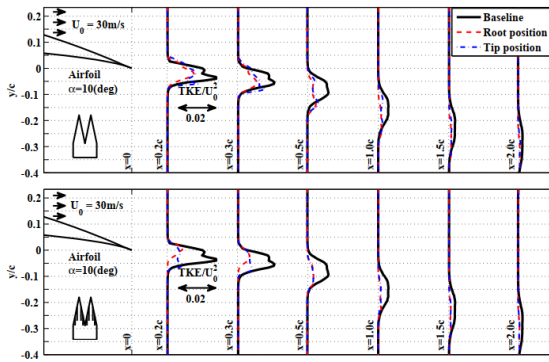


Figure 10

**Wake Turbulent Kinetic Energy for NACA 65(12)-10 Airfoil at  $\alpha=10^\circ$ . [8]**

**METHODOLOGY**

**Dimple Geometry**

To determine the position and dimension of the upper surface dimples, the following characteristics are required. The term  $\epsilon$  refers to the x-coordinate of the dimple's center relative to the chord line of the airfoil. To generate the dimple the terms  $r$  and  $h$  are used to define the radius and the depth of indentation, respectively. As the dimples will be applied along the entire span of the blade the term  $d$  will denote the center-to-center distance between each dimple (seen in Figure 11 and Figure 12).

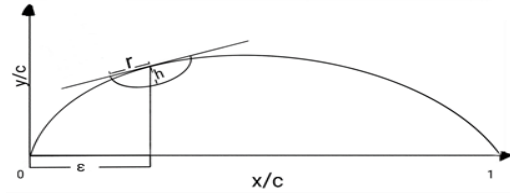


Figure 11

**Upper Surface Dimple Dimensions, Side View**

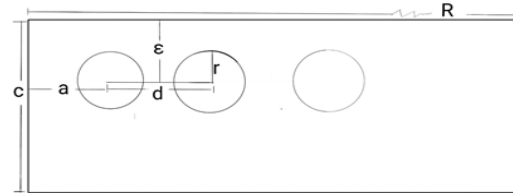


Figure 12

**Upper Surface Dimple Dimensions, Top View**

For the purposes of this project, the dimple characteristics will be fixed to:

$\epsilon = 30\%$  of the chord

$h = .1114\text{in}$

$r = .1856\text{in}$

$d = 1.5\text{in}$

$a = .75\text{in}$

**Flatback Conversion**

For this project, the flatback airfoils will be created by thickening the rear segment of the airfoil, past the maximum thickness point. This method provides a reduced pressure gradient along the airfoil compared to the original and maintains the camber line shape and thickness ratio, which is not the case on a truncated airfoil.

To transform the airfoil, the flatback profile equation will be used. This equation takes the original set of coordinates that define the selected profile and adds thickness pass a desired point in a symmetrical manner [10]:

$$\bar{y}^{fb} = \bar{y}^{or} \pm \frac{TE/100}{2} a(\bar{x}) \quad (1)$$

where:

$\bar{y}^{fb}$ : y-coordinate of flatback profile (non-dimensional)

$\bar{y}^{or}$ : y-coordinate of original profile (non-dimensional)

TE: Desired trailing edge thickness with respect to the chord (%)

$\bar{x}$ : x-coordinate of profile (non-dimensional)

$a(\bar{x})$ : Distribution factor (non-dimensional)

The distribution factor  $a(\bar{x})$  is a function that distributes the additional thickness along the chord length. The distribution factor is defined as:

$$a(\bar{x}) = A(\bar{x} - B)^n + C\bar{x} \quad (2)$$

The constants A, B, and C are computed by applying boundary conditions on the profile, which are the point where the thickness addition begins and the trailing edge. The parameter  $n$  is used to adjust the transition smoothness. It was tested to be smoothest when  $n = 0.5$  [11]. The term  $\varepsilon$  is used to denote the starting point along the x-axis from the leading edge where the thickness is added to the airfoil.

To set up the boundary conditions, a few conditions need to be met. It is desired that the distribution factor begins just after the point  $\varepsilon$  and finishes at the trailing edge. It is also desired that at point  $\varepsilon$  the distribution factor is parallel to the x-axis to ensure the thickness is added smoothly after the starting point. The boundary conditions are as follows:

$$\bar{x} = \varepsilon \rightarrow a = 0 \quad (3)$$

$$\bar{x} = 0 \rightarrow a = 1 \quad (4)$$

$$\frac{da}{d\bar{x}} = An(\bar{x} - B)^{n-1} + C = 0 \quad (5)$$

With these conditions, it is now possible to calculate the constants for  $a(\bar{x})$ :

$$A = \frac{1}{(1 - B)^n - n(\varepsilon - B)^{n-1}} \quad (6)$$

$$B = \varepsilon(1 - n) \quad (7)$$

$$C = 1 - A(1 - B)^n \quad (8)$$

For the present research, a script developed in MATLAB was used to generate the conversion. The input variables for the Flatback conversion are as follows:

$$TE = 4.2\% \text{ t/c}$$

$$\varepsilon = 29.9\% \text{ x/c}$$

$$n = 0.5$$

### Serration Geometry

The serration to be used in this project will be an M-Shaped trailing edge [12]. As the airfoil will possess a flatback shape, the trailing edge will have a thickness,  $h$ , which is the basis of the equations used to define the serration dimensions. The term  $b_1$  is the width of the separation between each M-shape and  $b_2$  is the width of the M-shape itself. The term  $a$  is the depth of the serration while  $\gamma$  is angle of the serration. Figure 13 illustrates the parameters for this geometry:

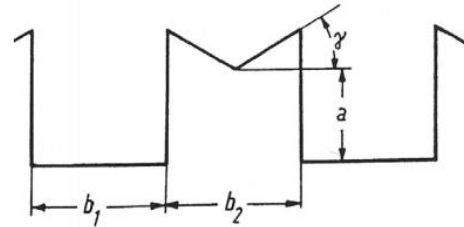


Figure 13

### Dimensions of M-shaped Serrated Trailing Edge [9]

The design is characterized by the optimizations that reduce the drag generated by the flatback shape

by 46%. [12] The optimized parameters are related as follows:

$$\frac{a}{h} = 1.9 \quad (9)$$

$$b_1 = b_2 = 3.66h \quad (10)$$

$$\gamma = 40^\circ \quad (11)$$

The serrations will be part of a splitter plate integrated into a flatback blade and will be aligned with camber of the blade. Effectively, it will be a 3mm plate protruding at an angle of 16.44° downwards.

### Wind Tunnel Testing

The wind tunnel used is a Flotek 1440, an open circuit system with a 12" x 12" x 36" test section with an airspeed of approximately 93 fps. The models are placed vertically inside the test section. A force balance is used to measure the lift and drag on the blade over a time interval of 15 seconds, taking the last 5 seconds for evaluation. Wind tunnel speed, lift and drag measurements of the 5 second interval are then averaged and tabulated. Each blade is tested three times from an angle of attack ranging from -15° to 30°. As we are assuming a standard atmospheric condition, the Reynolds Number will be around 296,000. All models were 3D printed with PLA, then progressively sanded down with 80, 150, 320, and 500 grit sandpaper. An aluminum insert was manufactured to fit inside the blades and threaded to hold the blade onto the force balance beam.

## RESULTS

Wind tunnel experimentation results are presented. Observing the control model was the first step; then compared the variations against the control. The dimpled variations with their smooth counterpart were compared too.

The S825 control blade's aerodynamic characteristics are shown in Figure 14 and Figure 15.

A linear behavior can be seen from -5° up to 8° with the maximum lift coefficient at 12°. The angle for zero lift occurs at -4.62°. A sudden lift coefficient drop is seen between 17° and 18°. For drag, a linear behavior is also seen from -2° up to 17°, when the drag coefficient increase occurs. Afterwards, the linear behavior continues with a slightly steeper slope. The effect of the sudden coefficient spike on drag is more pronounced compared to lift.

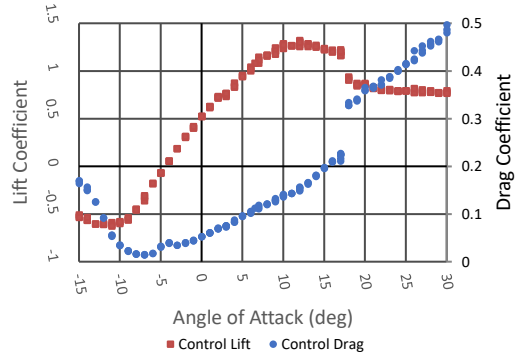


Figure 14

### Lift and Drag Curve for the Control Blade, Re = 2.95E5

When introducing the dimples to the control model, no significant differences can be observed. The linear region is near identical for both lift and drag. The angle where lift coefficient drop occurs is increased to 19° and the maximum lift coefficient is reduced by 5.88%.

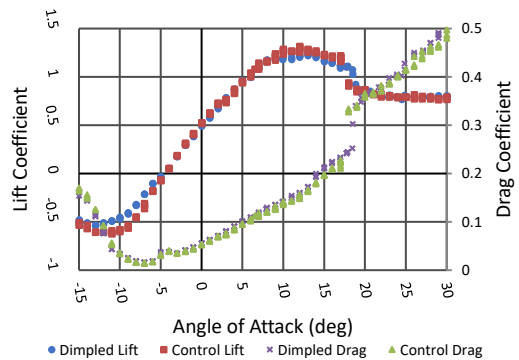


Figure 15

### Lift and Drag Comparison Between the Dimple Control Blade and the Control Blade, Re = 2.95E5

The Flatback modification to the S825 airfoil is effectively identical to the control model for both lift

and drag, main difference being in the lift coefficient drop occurring at higher angles between 19° and 20°.

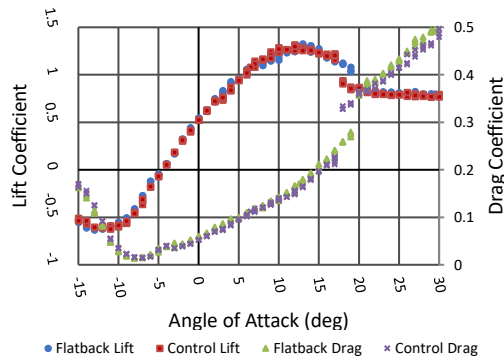


Figure 16

**Lift and Drag Comparison Between the Flatback Blade and the Control Blade,  $Re = 2.95E5$**

Introducing the dimples to the flatback design has increased the lift coefficient on positive angles of attack by a noticeable, yet not significant, average of 3.71%. However, the drag coefficient increases by an average of 10.28% over the control blade.

At near stall angles between 9° and 13°, the blade seems to be suffering from some form of instability, based on the fact that the data collected is not as consistent compared to the rest of the domain. The Flatback Dimple model also shares the characteristic with its smooth counter that the pressure drop occurs between angles of 19° and 20°. When comparing the two flatback designs with each other, the increase in lift reduces to 1.93% and drag coefficient increases to 5.94%. Both the Flatback blade and the Flatback Dimpled blade have similar aerodynamic behavior.

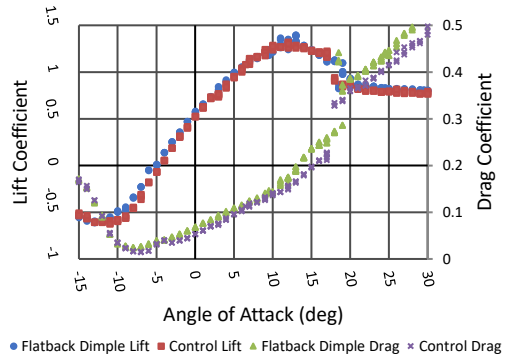


Figure 17

**Lift and Drag Comparison Between the Flatback Dimple Blade and the Control Blade,  $Re = 2.95E5$**

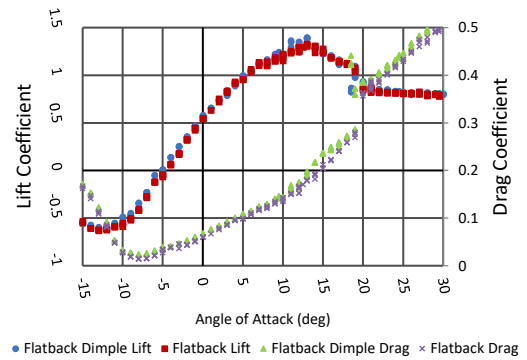
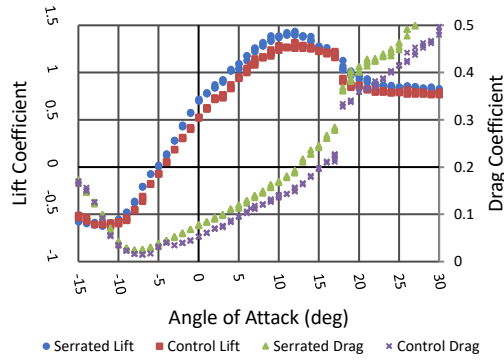


Figure 18

**Lift and Drag Comparison Between the Flatback Dimple Blade and the Flatback Blade,  $Re = 2.95E5$**

The M-shape serrations have markedly introduced an improvement in lift performance for an average of 7.43%, with the maximum lift increasing by 9.94% over the control. However, the drag coefficient has increased for an average of 22.62%. Interestingly, the pressure drop occurring at 17° does not have as pronounced an effect on the lift as it did on the previous blades. This drop can still be seen on the drag curve. The zero-lift angle serrated blade occurs at -5.56°, 16.14% further behind what was observed in the control blade.



**Figure 19**

**Lift and Drag Comparison Between the Serrated Blade and the Control Blade,  $Re = 2.95E5$**

Adding the dimples to the serrated blade does not significantly alter the aerodynamic performance to the blade. In comparison with the smooth serrated blade the average lift only increases by 0.77% while the drag increases by 4.79%. When compared to the control blade, lift and drag are increased by 12.6% and 31.55%, respectively, for positive angles. The maximum lift coefficient is 10% higher compared to the control blade, occurring at  $10.31^\circ$ .

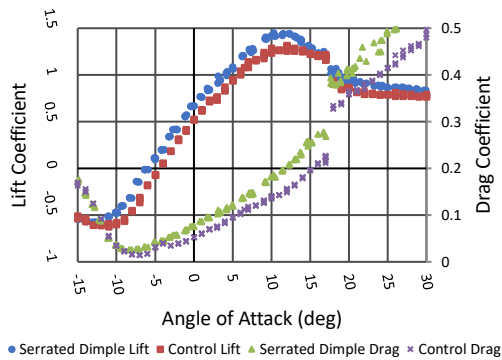


**Figure 20**

**Lift and Drag Comparison Between the Serrated Dimple Blade and The Control Blade,  $Re = 2.95E5$**

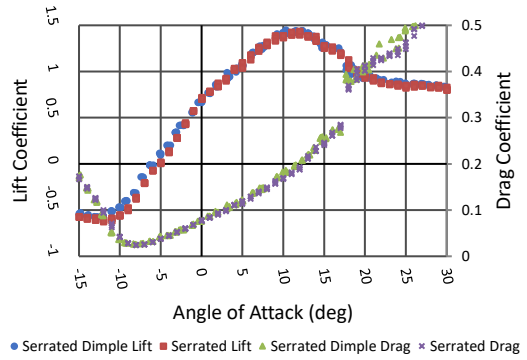


**Figure 21**

**Lift and Drag Comparison Between the Serrated Dimple Blade and the Serrated Blade,  $Re = 2.95E5$**

The following Table 1 organizes the main aerodynamic characteristics for each blade model, namely the Maximum lift coefficient and its angle, the zero-lift angle, and the maximum lift-to-drag ratio with its angle. In general, both Serrated blades and the Flatback dimple blade have improved maximum lift coefficient. Only the Serrated dimple blade has a noticeable reduction in the angle of maximum lift coefficient and the zero-lift angle. Due to the large increases in drag for all blade variations, the  $Cl/Cd_{max}$  of the control blade is the highest of the group. It does not appear that the dimples assist in the aerodynamic performance of the blades in this study; they only managed to increase drag. It also seems that the serrations used only increases drag by an average of 0.20% while reducing total lift by an average of 0.072% compared to the flatback design.

**Table 1**

**Aerodynamic Characteristics of Experimented Blades**

Model	Characteristic	$Cl_{max}$	$\alpha_{Cl_{max}}$	$\alpha_{Cl=0}$	$Cl/CD_{max}$	$\alpha_{Cl/CD_{max}}$
Control		1.32	12.00	-4.45	10.42	2.00
Control Dimple		1.24	13.00	-4.63	9.65	3.00
Flatback		1.33	13.00	-4.57	9.65	5.00
Flatback Dimple		1.39	13.00	-5.15	9.15	5.00
Serrated		1.44	12.00	-5.17	9.35	1.00

Serrated Dimple	1.45	10.31	-6.15	8.92	4.16
-----------------	------	-------	-------	------	------

Comparing all these blades, side by side, we get the following charts for lift and drag coefficients, Figure 22 and Figure 23 respectively. These charts are polynomial trendlines based on the data acquired during the experiments. As previously stated, we can see how similar the two Flatback models and the Control Dimple model are to the Control Blade and how much more lift is generated by the two Serrated models. We can also see that all increase in lift is accompanied by a larger increase in drag for each of the blades compared to the control.

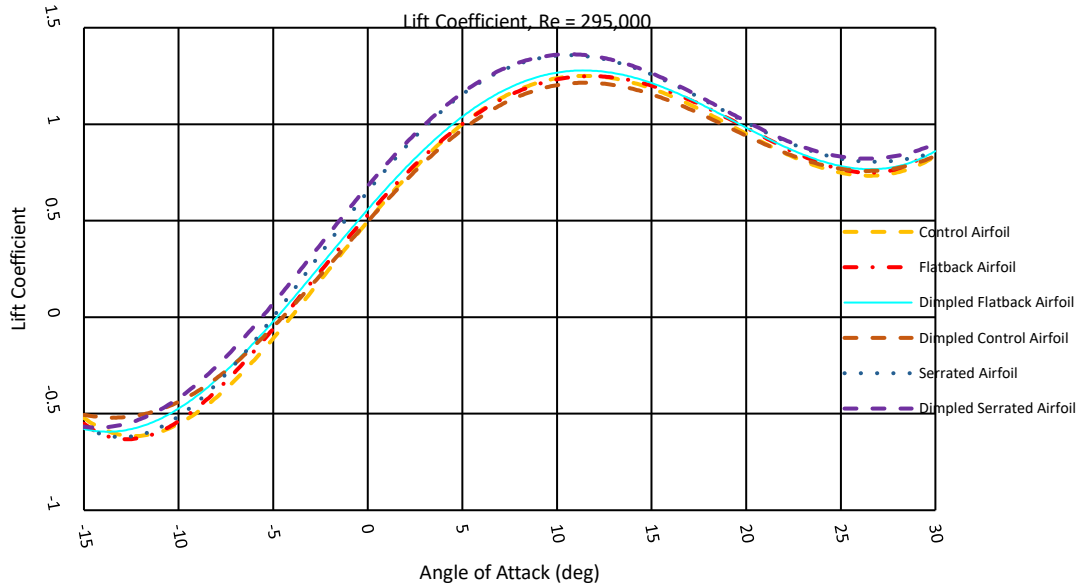


Figure 22

Trendlines for Lift Coefficient of All Experimented Blades

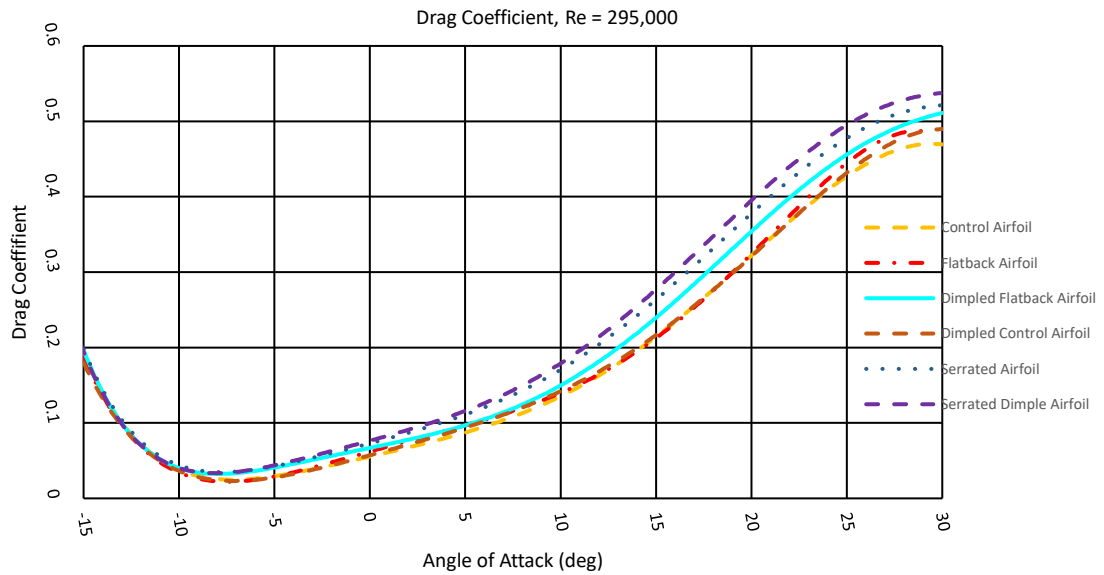


Figure 23

Trendlines of Drag Coefficient for All Experimented Blades

## DISCUSSION

The researcher speculates that the position of the upper surface dimples is one of the major causes of unexpected results. These dimples were placed far forward on the chord line, right where

the maximum thickness of the airfoil occurs. Flow separation does not occur near this area when reaching the maximum lift angle; therefore, the recirculation provided by the dimples does not impact the boundary layer. The thickness of the

serrations might also have negatively affected the results of the experiments. Both of these features should demand further investigation.

The original objective of this experiment was to improve the aerodynamic characteristics of a wind turbine blade by introducing modifications to the upper surface and to the trailing edge of the blade. During the course of the study, the investigator found that these modifications did not improve the lift performance of the blade enough to justify the increase of drag that has been observed. The serration geometry studied seems to not have any drag improvements over a flatback airfoil. The dimpled implemented on each blade did little action to reenergize the flow.

The investigator believe that research into the dimples should be more focused in varying the geometry and size of the dimple, the height or depth of indentation, the angle of these shapes relative to the flow direction, their pattern geometry, and their positioning relative to the chord line. These future works will be attended in the aerodynamic laboratory of the PUPR.

## REFERENCES

- [1] J. Scott, "Ask Us - Golf Ball Dimples & Drag," 13 February 2005. [Online]. Available: <http://www.aerospaceweb.org/question/aerodynamics/q0215.shtml>. [Accessed July 19, 2019].
- [2] S. S. Mahamuni, "A Review on Study on Aerodynamic Characteristics of Dimple Effect on Wing," *International Journal of Aerospace and Mechanical Engineering*, vol. 2, no. 4, July 2015.
- [3] E. Livya, G. Anitha and P. Valli, "Aerodynamic Analysis of Dimple Effect on Aircraft Wing," *International Journal of Mechanical, Aerospace, Industrial, Mechatronic and Manufacturing Engineering*, vol. 9, no. 2, pp. 350-353, 2015.
- [4] M. Mashud, D. Mondal and M. E. Haque, "Experimental Investigation of Airfoil with Multiple Dimples on the Upper Surface," in *International Conference of Mechanical Engineering and Renewable Energy*, Chittagong, Bangladesh, 2017.
- [5] X. Y. Wang, S. Lee, P. Kim and J. Seok, "Aerodynamic Effect of 3D Pattern on Airfoil," *Transactions of the Canadian Society for Mechanical Engineering*, vol. 39, no. 3, pp. 537-545, 2015.
- [6] C. v. Dam, "Airfoils for Structures - Passive and Active Load Control for Wind Turbine Blades," in *Sandia Blade Workshop*, Albuquerque, 2004.
- [7] J. Mathew, A. Singh, J. Madsen and C. A. León, "Serration Design Methodology for Wind Turbine Noise Reduction," *Journal of Physics: Conference Series*, September 2016.
- [8] X. Liu, M. Azarpeyvand and R. Theunissen, "On The Aerodynamic Performance of Serrated Airfoils," in *The 22nd International Congress on Sound and Vibration*, Florence, Italy, 2015.
- [9] X. Liu, H. K. Jawahar and M. Azarpeyvand, "Wake Development of Airfoils with Serrated Trailing Edges," 2016.
- [10] O. C. Seix, "Aerodynamic study on the design and optimization of flatback airfoils for wind turbine applications," Barcelona, 2015.
- [11] E. S. Ferry, "Estudio aerodinámico y optimización de perfiles flatback aplicado a aerogeneradores.," Universitat Politècnica de Catalunya, 2014.
- [12] C. v. Dam, D. L. Kahn and D. E. Berg, "Trailing Edge Modifications for Flatback Airfoils," Sandia National Laboratories, Albuquerque, 2008.